18TH WORLD CONFERENCE ON EARTHQUAKE ENGINEERING
WCEE2024
MILAN

MILAN, ITALY
30TH JUNE - 5TH JULY 2024

www.wcee2024.it

STATE-DEPENDENT SEISMIC FRAGILITY FUNCTIONS FOR VERTICAL TANKS INSTALLED ON MAJOR HAZARD INDUSTRIAL SUBSTRUCTURE MODULE

C. Nardin[1*], O.S. Bursi[1], M. Broccardo[1], S. Marelli[2], B. Sudret[2]

[*] University of Trento – Department of Civil, Environmental and Mechanical Engineering, Trento, Italy, chiara.nardin@unitn.it

University of Trento – Department of Civil, Environmental and Mechanical Engineering, Trento, Italy

[2] ETH Zürich - Department of Civil, Environmental and Geomatic Engineering – Chair of Risk, Safety and Uncertainty Quantification, Zürich, Switzerland

Abstract: *Seismic vulnerability assessment of industrial plants and process equipment has gained attention lately. However, the complexity of the problem and its modelling, combined with a general scarcity of available data on industrial systems, contributed to limiting or developing risk assessment methods based on extremely simplified models. On these premises, a new methodology that combines limited data from finite element FE models with cutting-edge machine learning techniques is developed to generate state-dependent fragility functions for critical components mounted on archetypical industrial substructure modules. Specifically, referring to the classical forward uncertainty quantification scheme, a physics-informed FE model, calibrated on the results of a comprehensive shake table test campaign of a real-scale industrial braced-frame BF steel substructure, is considered. Time histories of seismic event sequences generated by a site-based ground motion model compose the input provided to the FE model. The uncertainty is then propagated through Monte Carlo analysis on inexpensive-to-run polynomial chaos expansion (PCE) metamodels set for each starting damage level condition measure. As a result, empirical state-dependent fragilities are evaluated, assuming the lognormal distribution.*

1. Introduction

1.1. Background and literature review

Structural and non-structural components vulnerability is a crucial step for risk assessment, see Du et al. (2021). This holds true, especially for major hazard industrial facilities in seismic-prone zones. Over the last decade, the PEER Performance-Based Earthquake Engineering (PBEE) framework has become the most widespread tool for estimating risks. Versatility and modularity characterised the PEER methodology. Precisely, it builds on the application of the total probability theorem at each stage of risk assessment. Thus, it enables to analyse separately the (i) seismic hazard, (ii) fragility, (iii) damage and (iv) loss phases, and, thus, to recombine them together as a function of a specific decision variable metric. In this context, the focus is on the fragility analysis step. Fragility or vulnerability analyses represent the bridge between seismic hazard and structural modelling. They provide the conditional probability of overpassing damage state (DS) thresholds, given a seismic input. Initially introduced for nuclear safety evaluation by Richardson et al. (1980), fragility curves are now widely employed. They range from loss estimation as in Rossi et al. (2020) to assessing collapse risk, see Eads et al. (2013), quantifying resilience at the individual and community levels as in Cimellaro et al. (2010) – Burton et al. (2016), and more.

Recently, research shifted towards state-dependent fragility functions. These enable to model the probability of exceeding damage thresholds conditioned not only by seismic hazard, but also by initial damage state conditions. Iervolino et al. (2015) provides a pioneering example applied to simple equivalent single-degree-of-freedom systems. However, to tackle more complex systems, as in the work of Ghosh and Padgett (2010), the computational and time burden becomes non-negligible. In this respect, surrogate modelling alleviates the issue. Du and Padgett (2020), Abbiati et al. (2021), Gentile and Galasso (2020) investigate different surrogate, or metamodeling, techniques, ranging among artificial neural networks, hierarchical Kriging and Gaussian processes, respectively, to perform seismic fragility assessment.

In addition, in the development of state-dependent fragility functions, the seismic input plays a relevant role. To mimic the effects of ageing and damage accumulation on structures due to the impact of multiple seismic events in the lifespan of a structure, sequential seismic time series become a crucial element in accurate risk assessment. Abdelnaby (2018), Kassem et al. (2019) thoroughly investigated the cumulative effect of damage accumulation and disruption caused by sequences of earthquakes, such as those in Wenchuan (2008), Tohoku (2011), and central Italy (2016). Moreover, Zhang et al. (2018) provide insights on how to properly select record pairs for sequential response non-linear time history analysis (NLTHA). They recommend seismic sequences that comprise both main-shock (MS) and after-shock (AS) record pairs to capture and maintain within-sequence correlations.

At the same time, the USA National Institute of Standards and Technology released a year-long comprehensive study, NIST (2017), on the seismic behaviour and performances of non-structural components (NSCs) in civil and industrial structures. Its relevance stems from their role as the primary contributors to direct losses resulting from earthquake damage, see the research of De Biasio et al. (2015) and Nardin et al. (2022). Thus, NSCs in industrial plants have been identified as a top priority in seismic risk assessment.

However, limited real-world case studies and experimental test data are available for complex industrial systems, Butenweg et al. (2020, 2021). Additionally, also numerical non-linear dynamic analyses considering coupling interactions between NSCs and the main structure represent an open challenge, severely constrained by computational resources. Moreover, conducting a full probabilistic fragility analysis is strictly limited by the computational feasibility of performing a sufficiently large number of NLTHAs. Nonetheless, this challenge perfectly aligns with the classical problem in simulation-based uncertainty quantification (UQ), which is mitigated by replacing the computationally intensive NLTHAs with an equivalent surrogate model, as demonstrated in Sudret (2007).

Undoubtedly, one of the most significant advantages of employing surrogate models is the ability to gather an extensive amount of data and conduct analyses at a minimal cost. This facilitates the creation of empirical fragility functions, as demonstrated in the literature by Global Earthquake Model (GEM) which can then be compared with the commonly used assumption of a lognormal distribution.

1.2. Scope and core contribution

On these premises, the paper presents an innovative methodology for state-dependent fragility function analysis. Indeed, the methodology combines limited data from finite element FE models with cutting-edge machine learning techniques. Specifically, building on the classical UQ forward analysis scheme, it enables the fragility analysis of a vertical tank installed on a steel frame industrial substructure by metamodeling via polynomial chaos expansion (PCE) the seismic response of the component's FE model. The paper is organised as follows. Section 2 illustrates the innovative state-dependent methodology; whilst in Section 3 the fragility analysis for the vertical tank mounted on the shake table tested steel structure is presented. Lastly, Section 4 collects the relevant conclusions and drafts future research perspectives.

2. State-dependent fragility framework

State-dependent fragilities are defined as those functions conditioned not only by a measure of seismic intensity (IM) but also by the initial state of damage DS_i in which the structure lies, see Iervolino et al. (2015).

Hence, state-dependent fragilities allow to assess the vulnerability of a system that could have already experienced or be in a certain range of damage, as defined by the generalised Eqn. 1:

$$\mathbb{P}[\mathrm{DS_j}\,|\mathrm{DS_i}, \mathrm{IM} = \mathrm{im}] = \mathbb{P}[\mathrm{DS} \geq \mathrm{DS_j}\,|\mathrm{DS_i}, \mathrm{IM} = \mathrm{im}] - \mathbb{P}[\mathrm{DS} \geq \mathrm{DS_{j+1}}|\mathrm{DS_i}, \mathrm{IM} = \mathrm{im}] \quad (1)$$

for $j > i$ and i index ranging among the identified and most severe damage limit states. The possible transitions between damage states are schematically represented in Figure 1. Moreover, in Figure 1 the generalised transition probability state matrix for a system with a three-level damage state metric, i.e., DS_0-DS_1-DS_2, is reported. Each row of the matrix represents the initial damage level state; whilst each column indicates the transition to or the residency into a damage state condition. The lower triangular matrix represents the recovery processes of the investigated system, not considered here. Moreover, the ultimate damage limit state is considered an absorption state, i.e., a condition that, once reached, cannot be exited. This reflects the collapse case of the structural system.

In the proposed state-dependent innovative framework, the empirical fragility functions are evaluated via Monte Carlo method applied to metamodels for the different initial damage state conditions.

The theoretical backbone of the framework lies in the UQ forward method analysis developed by Sudret (2008). According to the authors, three steps, i.e., A-B-C, describe how to deal with any UQ problem. First, i.e. step A, the computational model – numerical, analytical or FE – needs to be defined. Then, the input and model parameters are defined. Lastly, uncertainties are propagated through Monte Carlo forward analysis. Post-processing of the quantity of interests (QoIs) is then performed. Specifically, to derive state-dependent fragility functions, the scheme depicted in Figure 2 is pursued.

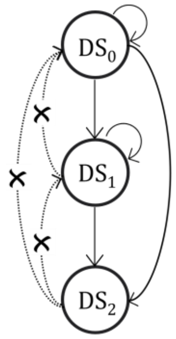

Initial damage state DS_i \ Transition to damage state DS_i	$\mathbf{DS_0}$	$\mathbf{DS_1}$	$\mathbf{DS_2}$
$\mathbf{DS_0}$	$1 - \mathbb{P}_{01} - \mathbb{P}_{02}$	$\mathbb{P}[DS \geq DS_1 \mid DS_0, IM] - \mathbb{P}[DS \geq DS_2 \mid DS_0, IM]$	$\mathbb{P}[DS \geq DS_2 \mid DS_0, IM]$
$\mathbf{DS_1}$	×	$1 - \mathbb{P}_{12}$	$\mathbb{P}[DS \geq DS_2 \mid DS_1, IM]$
$\mathbf{DS_2}$	×	×	1

Figure 1. Transition state diagram and matrix for state-dependent fragility analysis.

The assumed computational model (Step A) is the expensive non-linear (physics-informed) FE model of the SPIF experimental campaign, illustrated in Subsection 3.1. Then, in Step B, the input and uncertainties of the model parameters are set. Specifically, a site-based ground motion model (GMM) is deployed to generate a huge ensemble of synthetic ground motions. From this ensemble, seismic events are sampled to reproduce suitable seismic time history sequences (STHS), more details in Subsection 3.2. Non-linear STHS analysis are performed. The resulting time history of response of the considered QoI is then classified and clustered according to the damage limit state metric. Thus, different experimental design $\mathcal{E}_s = \{(\mathcal{X}^{(i)}, \mathcal{Y}^{(i)}) : \mathcal{Y}^{(i)} = g(\mathcal{X}^{(i)}) \in \mathbb{R},\ i = 1, ..., N\}$ are set for each identified s-initial damage state condition. To reduce the input dimensionality, principal component analysis (PCA) is applied to the ground motions. PCE metamodels are developed for each set of experimental design and Monte Carlo analysis are performed. Lastly, based on the PCE simulations' results, empirical state-dependent fragilities are computed as terms of the generalised transition state probability matrix of Figure 1.

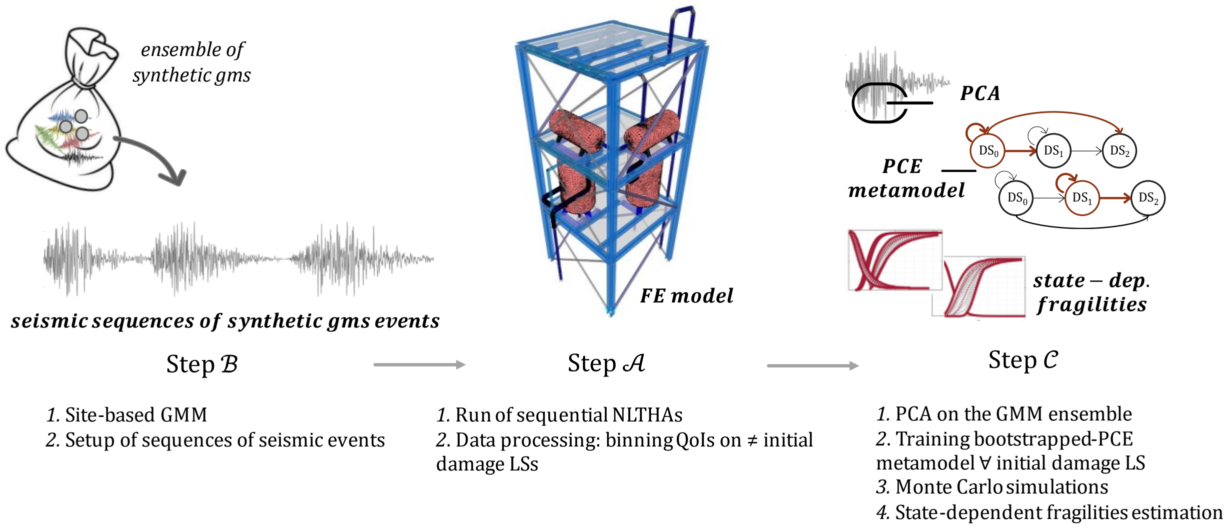

Figure 2. State-dependent fragility analysis UQ-based framework.

3. Application to an industrial process component

In this Section, the proposed framework for state-dependent fragilities is applied to a critical process component, e.g., a vertical tank, mounted on an archetypal industrial braced frame (BF) steel substructure of the experimental shake table test campaign SPIF #2. The required steps, i.e., A-B-C, for the UQ framework are thoroughly presented in next Subsections.

3.1. Step A: the FEM of SPIF#2

The reference FE model for the analysis is the one developed for the recent SPIF #2 project, see Butenweg et al. (2020). The project SPIF, i.e., Seismic Performance of Industrial Facilities, consisted of comprehensive shake table tests carried out at EUCENTRE Laboratory, Italy. The tested mock-ups were true-scale industrial steel frame structures - moment-resisting and braced frames, SPIF and SPIF #2, respectively - equipped with process components such as bolted flange joints, pipes, electrical cabinets, a conveyor, and vertical and horizontal tanks.

Figure 3(a) depicts the expensive 3D FE model of the SPIF #2 experimental tests campaign. Briefly, the mock-up consists of a full-scale 3-storey steel BF structure with flexible floors and process components mounted on.

During the campaign, the complex dynamic interaction between the main steel structure and the vertical tanks installed on the first level of the structure was of particular interest. Figure 3(b) reports a close-up photo of one of the two vertical tanks. Hence, careful consideration was paid to the FE modelling for those components. In this respect, Figure 3(c) depicts a detail of the ad-hoc designed stick model for the tanks. The stick model was developed by a reference high-fidelity FE model of the vertical tank with the twofold goals to: (i) mimic the modal properties and (ii) catch the different effects of the participating seismic mass on the supporting girders system, related to the intensity level of the seismic excitation. A thorough discussion on FE modelling and calibration of the SPIF #2 mock-up can be found in Nardin et al. (2022), Quinci et al. (2023).

Hence, state-dependent fragility analysis is applied on this process component. According to the industry standards and collected data from the extensive experimental campaigns, two limit states are identified. The first is linked to the operation and functionality of the process plant, namely the Design Basis Earthquake (DBE); the second is related to the safe shutdown conditions, thus called Safe Shutdown Earthquake (SSE). Thresholds are formulated in terms of maximum acceleration recorded at the base of the tank: 6.72 $\mathrm{m/s^2}$ is the limit threshold for the DBE condition and 18.5 $\mathrm{m/s^2}$ for the SSE, respectively.

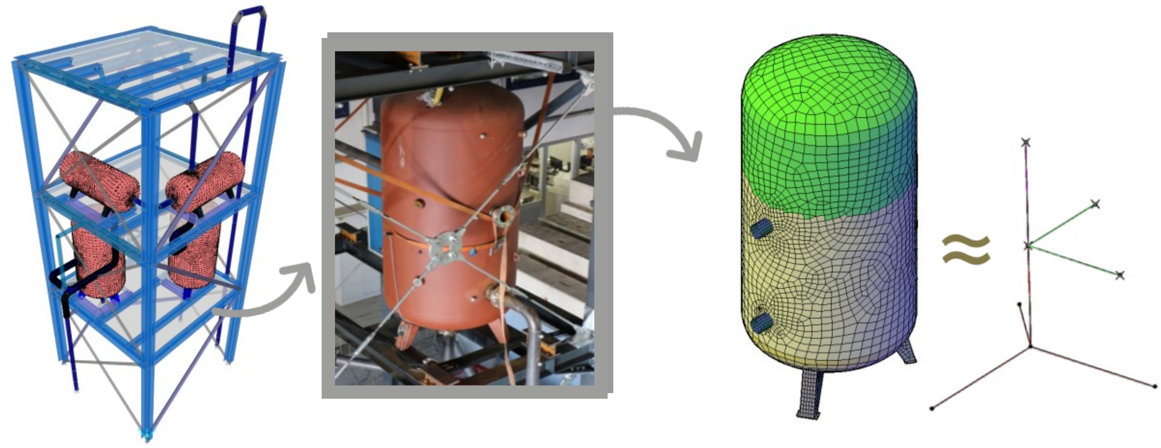

(a) (b) (c)

Figure 3. (a) BF full FE model of the SPIF#2 mock-up. (b) Photo, (c) high-fidelity FE and stick models for the critical installed vertical tank, respectively.

3.2. Step B: the time series of seismic sequence events

The site-based GMM of Rezaeian and Der Kiureghian (2010) was employed to generate an ensemble of 10^4 synthetic ground motions (gms). The parameters of the GMM were inferred from a dataset of natural records of a severe seismic-prone zone in the centre of Italy. Table 1 collects the parameters of the GMM.

Table 1. Probabilities density distributions of the parameters of the site-based GMM.

Model Parameters	Units	Distribution	μ	σ	Distribution Bounds
I_a – Arias Intensity	[m/s]	Log-normal	-0.46	0.51	(0; +∞)
D_{5-95} – Time interval of 95% of the I_a	[s]	Log-normal	2.21	0.23	(0; +∞)
t_{mid} – Time interval of 45% of the I_a	[s]	Log-normal	1.70	0.21	(0; +∞)
$\omega_{mid}/2\pi$ – Filter frequency at t_{mid}	[Hz]	Uniform	4.80	1.00	[3.80;5.80]
ζ_f – Filter damping ratio	[-]	Uniform	0.35	0.10	[0.25;0.45]

**$\dot{\omega}_{mid}$, rate of change of frequency with t, constant and equal to -0.5*

Out of them, gms were randomly sampled to constitute sequences of seismic events to assign as input for the fragility analysis. Those multiple shocks are sequences of main-shock events only. This choice is legit since it is assumed that no retrofit or recovery interventions happen between two seismic events and the ageing effects on the structure are negligible.

Hence, the generated main-shock seismic sequences are assigned as input to the FE models. However, because of the prohibitive computational cost of performing NLTHAs, only a few numbers (~150) of full non-linear analysis are performed. The results of those simulations are clustered based on the initial damage state of the system, as schematically depicted in Figure 4. Thus, ---results-input gms---- pairs are collected in separated datasets that constitute the experimental design $\mathcal{E}_s$ for the PCE metamodels. Each initial damage state condition represents a different PCE surrogate model. Therefore, three different experimental design $\mathcal{E}_0$, $\mathcal{E}_1$, $\mathcal{E}_2$ are derived: they represent the rows of the transition matrix of Figure 1.

Lastly, to reduce the input dimensionality for the PCE metamodels, principal component analysis is performed on 42 characteristic IMs of the gms. As a result, PCE is performed on the first six principal components (PCs) that cover almost the 90% of the input variability.

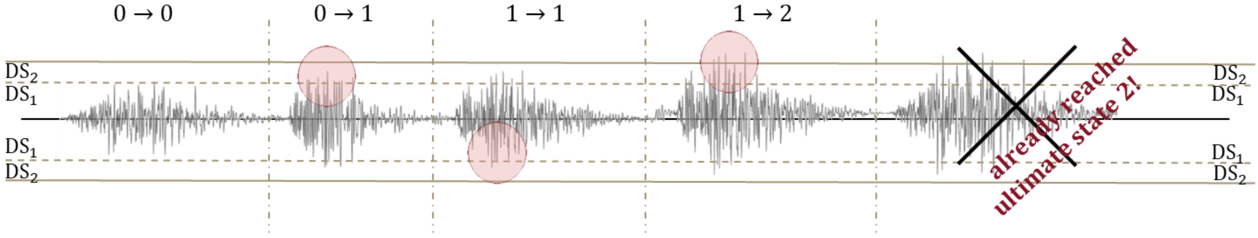

Figure 4. Clustering of QoIs simulations' results, according to a three-state - DS_0, DS_1, DS_2 - damage metric.

3.3. Step C: Monte Carlo simulations for state-dependent fragilities

PCE provides a functional approximation of a computational model $\mathcal{M}(\underline{\mathcal{X}})$ through its spectral representation on a suitably built basis $\psi_\alpha(\underline{\mathcal{X}})$ of polynomial functions, see Marelli et al. (2022). Due to limited computing power, the bases are truncated and the governing equation becomes:

$$\mathcal{Y} = \mathcal{M}(\underline{\mathcal{X}}) \simeq \mathcal{M}^{PCE}(\underline{\mathcal{X}}) = \sum_{\alpha\in\mathcal{A}} c_\alpha \psi_\alpha(\underline{\mathcal{X}}) \quad (2)$$

Hence, it enables to drastically reduce the computational time to perform simulations. This allows to perform the Monte Carlo analysis for state-dependent fragility curves.

Specifically, two different surrogate models are calibrated for the two sets of initial damage state conditions, i.e., DS_0 -pristine and DS_1 damaged – the first two rows of the transition matrix of Figure 1.

Several combinations of size of the experimental design $\mathcal{E}_s$ and different solvers were tested. Based on three different measures of model error, i.e., the relative generalisation ε_{gen}; the leave-one-out ε_{LOO} and the empirical ε_{emp} error, an optimal dimension of the $\mathcal{E}_s$ was identified in 125 sample. As solver, the subspace pursuit SP was the one performing better for both the experimental design datasets. A thoroughly description of the procedure for selecting the solver and the required number of samples for the $\mathcal{E}_s$ is discussed in Nardin et al. (2024).

Hence, the estimation of the PCE coefficients for the pristine DS_0 initial condition converged at a polynomial degree 8 with $\varepsilon_{LOO} \simeq 0.08$. Figure 5 reports the histograms and validation $Y^{true} - Y^{PCE}$ plots. A validation set of 10^4 samples is deployed. A good agreement in terms of matching distributions between $Y^{true} - Y^{PCE}$ is reached; also, samples-pairs are neatly aligned on the 45^o line of the $Y^{true} - Y^{PCE}$ plot, indicating a favourable performance.

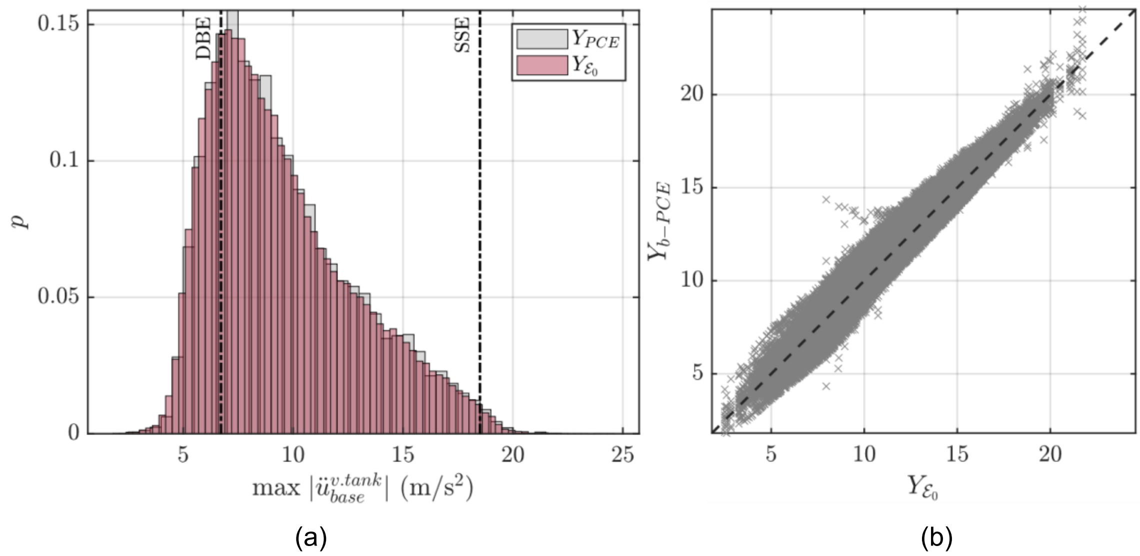

Figure 5. (a) Comparison of the histograms for the outputs, Y^{PCE}, of the PCE metamodel and the EDPs, Y^{true}, of the $\mathcal{E}_0$ dataset, i.e., the initial damage state condition DS_0. (b) Validation $Y^{true} - Y^{PCE}$ plot.

Similarly, Figure 6 reports the results of the validation of the PCE for the damage initial condition DS_1. The estimation of the PCE coefficients converged at a polynomial degree 8 with $\varepsilon_{LOO} \simeq 0.07$. The histograms and validation $Y^{true} - Y^{PCE}$ plots are represented. Anew, a good agreement in terms of matching distributions between $Y^{true} - Y^{PCE}$ is reached. Samples-pairs are well-aligned on the on the 45^o line of the $Y^{true} - Y^{PCE}$ plot, too.

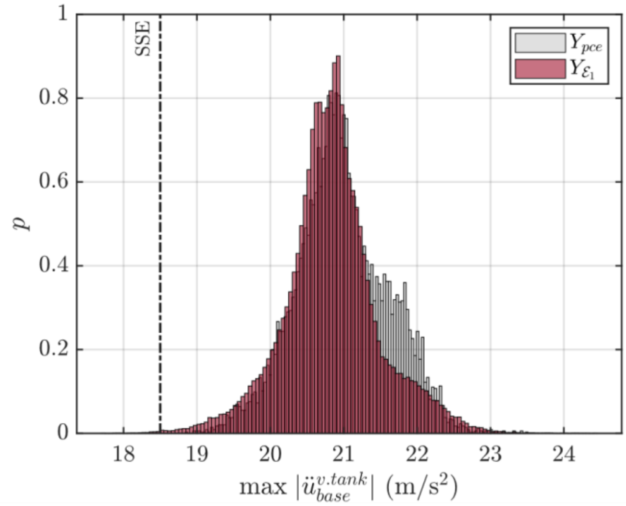

(a)

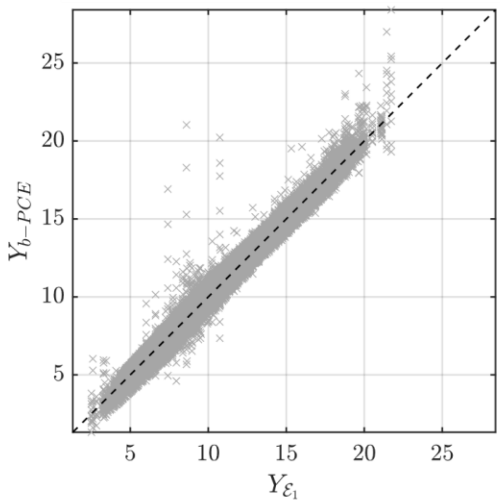

(b)

Figure 6. (a) Comparison of the histograms for the outputs, Y^{PCE}, of the PCE metamodel and the EDPs, Y^{true}, of the $\mathcal{E}_1$ dataset, i.e., the initial damage state condition DS_1. (b) Validation $Y^{true} - Y^{PCE}$ plot.

Hence, it is possible to derive state-dependent fragility functions by evaluating the Eqn. 1 on the outputs of the PCE metamodels. Empirical or nonparametric fragility analysis is performed, therefore, the bias induced by an a priori fixed distribution assumption is avoided.

As a result, Figure 7 gathers the state-dependent fragilities for the vertical tank of the SPIF #2 mock-up as function of the peak ground acceleration (PGA). Given an initial state damage level, the fragility curves associated to overpassing more severe limit states (DS_0, DS_1) are shifted to the left, e.g., the probabilities of damage increase with the level of the PGA. Instead, switching to the next initial damage level condition, the IM associated to the probability of overpassing limit state thresholds decreases. For example, fixed a column of the transition matrix -as the third column-, the same probability 0.50 of exceedance is reached for a PGA level of 4 m/s^2 for DS_0 initial condition and of 2.5 m/s^2 for DS_1 initial condition.

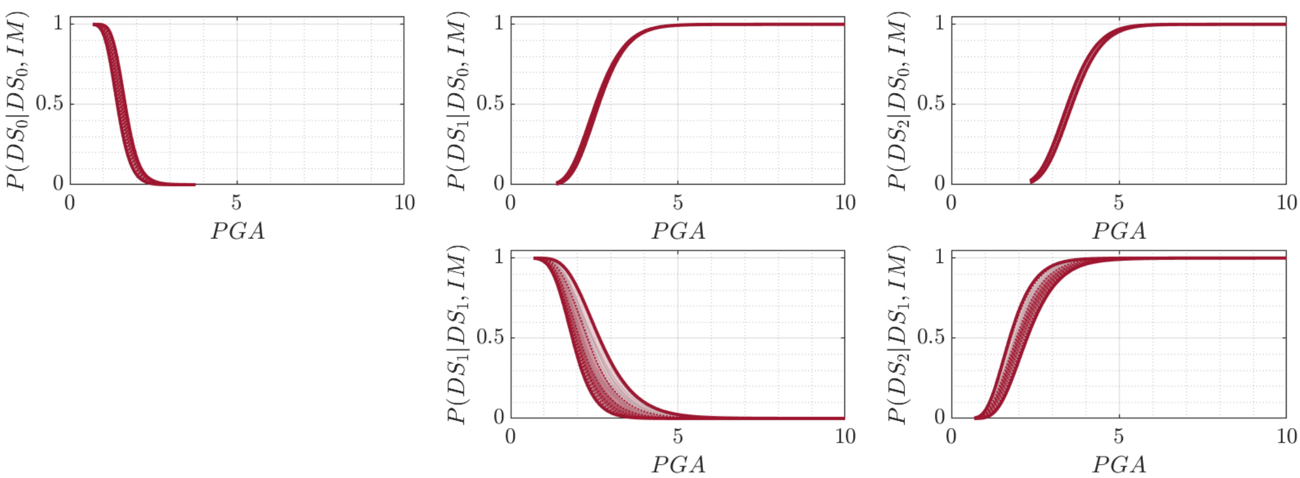

Figure 7. State-dependent fragility functions for the vertical tank of SPIF #2.

4. Conclusions and future developments

A new framework for state-dependent fragility analysis is proposed and tested on a real industrial component case study. The innovative framework combines limited data from finite element FE models with cutting-edge machine learning techniques. Specifically, driven by the classical forward UQ scheme, it enables to perform the huge number required for fragility analysis by leveraging PCE surrogate models.

The proposed methodology is tested on a critical component of the industrial shake-table tested mock-up SPIF - Seismic Performance of Industrial Facilities – project. The acceleration level at the base of the vertical tank installed on the first level of the SPIF's braced frame steel structure is considered as QoI for the state-dependent fragility analysis. Sequence of synthetic ground motions are generated and served as input for NLTHAs on the expensive to run computational FE model. Then, results of simulations are clustered in different experimental design dataset, according to the initial damage condition level metric. Separately, on experimental design a surrogate PCE model is developed. To overcome the input dimensionality burden, PCA is first applied to the seismic input of the PCE metamodeling. Monte Carlo analysis is performed by leveraging the metamodels. Thus, empirical state-dependent fragilities are evaluated. Those results pave the way for future investigations on the optima either parametric probability distribution or IM selection for state-dependent fragilities. Moreover, the possibility to quickly develop transition state matrix constitutes a first milestone towards the development of recovery functions for complex industrial systems.

5. References

Abbiati G, Broccardo M, Abdallah I, Marelli S, Paolacci F. (2021). Seismic fragility analysis based on artificial ground motions and surrogate modeling of validated structural simulators. *Earthquake Engineering & Structural Dynamics*. 50(9):2314-2333. 10.1002/eqe.3448

Abdelnaby, A. (2018). Fragility Curves for RC Frames Subjected to Tohoku Mainshock-Aftershocks Sequences. *Journal of Earthquake Engineering*, 22 (5), 902-920. 10.1080/13632469.2016.1264328

Burton H.V., Deierlein G., Lallemant D., Lin T. (2016). Framework for Incorporating Probabilistic Building Performance in the Assessment of Community Seismic Resilience. *Journal of Structural Engineering*, 142(8): C4015007. 10.1061/(ASCE)ST.1943-541X.0001321

Butenweg C. et al. (2020). Seismic performance of multi-component systems in special risk industrial facilities. Deliverable D10.1, SERA Project, Project. No: 730900, H2020-EU.

Butenweg C., Bursi O. S., Paolacci F., Marinković M., Lanese I., Nardin C., Quinci G. (2021). Seismic performance of an industrial multi-storey frame structure with process equipment subjected to shake table testing. *Engineering Structures*, 243, 112681.

Cimellaro G, Reinhorn A, Bruneau M. (2010). Framework for analytical quantification of disaster resilience. *Engineering Structures*, 32: 3639-3649. 10.1016/j.engstruct.2010.08.008

De Biasio M, Grange S, Dufour F, Allain F, Petre-Lazar I. (2015) Intensity measures for probabilistic assessment of non-structural components acceleration demand. *Earthquake Engineering & Structural Dynamics*, 10.1002/eqe.2582

Du A., Cai J., Li S. (2021). Metamodel-based State-dependent Fragility Modeling for Markovian Sequential Seismic Damage Assessment. *Engineering Structures*, 243. 10.1016/j.engstruct.2021.112644.

Du A., Padgett J. (2020). Investigation of multivariate seismic surrogate demand modeling for multi-response structural systems. *Engineering Structures.* 207. 10.1016/j.engstruct.2020.110210

Eads L, Miranda E, Krawinkler H, Lignos D. (2013). An efficient method for estimating the collapse risk of structures in seismic regions. *Earthquake Engineering & Structural Dynamics*, 42. 10.1002/eqe.2191

Gentile R, Galasso C. (2020). Gaussian process regression for seismic fragility assessment of building portfolios. *Structural Safety*. 87. 10.1016/j.strusafe.2020.101980

Ghosh J., Padgett J. (2010). Aging Considerations in the Development of Time-Dependent Seismic Fragility Curves. *Journal of Structural Engineering*. 136. 10.1061/(ASCE)ST.1943-541X.0000260

Iervolino I, Giorgio M, Chioccarelli E. (2015). Markovian modeling of seismic damage accumulation. *Earthquake Engineering & Structural Dynamics*, 45: 441–461. doi: 10.1002/eqe.2668

Kassem M.M., Nazri F.M., Wei L.J., Tan C.G., Shahidan S., Zuki S.S.M. (2019). Seismic fragility assessment for moment-resisting concrete frame with setback under repeated earthquakes. *Asian Journal of Civil Engineering.* 20: 465-477.

Marelli S, Lüthen N, Sudret B. (2022). UQLab user manual – Polynomial chaos expansions. tech. rep., Chair of Risk, Safety and Uncertainty Quantification; ETH Zurich, Switzerland. Report UQLab-V2.0-104.

Nardin C, Bursi OS, Paolacci F, Pavese A, Quinci G. (2022). Experimental performance of a multi-storey braced frame structure with non-structural industrial components subjected to synthetic ground motions. Earthquake Engineering & Structural Dynamics, 51(9): 2113-2136. 10.1002/eqe.3656

Nardin C., Marelli S., Sudret B., Bursi O.S., Broccardo M. (2024). Metamodel state-dependent fragility functions for non-structural components in special risk industrial facilities. *Under submission*

NIST (2017). *GCR 17-917-44. Seismic Analysis, Design, and Installation of Nonstructural Components and Systems*, National Institute of Standards and Technology, Gaithersburg.

Quinci G, Nardin C, Paolacci F, Bursi O. (2023). Modelling issues in seismic risk analysis of Non-Structural Components located on industrial plant subsystems. *Bulletin Earthquake Engineering*. 10.1002/eqe.1132

Rezaeian S, Der Kiureghian A. (2010). Simulation of synthetic ground motions for specified earthquake and site characteristics. *Earthquake Engineering & Structural Dynamics*. 10.1002/eqe.997

Richardson J., Bagchi G., Brazee R. (1980). The seismic safety margins research program of the US Nuclear Regulatory Commission. *Nuclear Engineering and Design*, 59(1): 15-25.

Rossetto T, Ioannou I, Grant D. (2015). Existing Empirical Fragility and Vulnerability Functions: Compendium and Guide for Selection. *GEM Technical Report*. 10.13117/GEM.VULN-MOD.TR2015.012

Rossi L, Stupazzini M, Parisi D, Holtschoppen B, Ruggieri G, Butenweg C. (2020). Empirical fragility functions and loss curves for Italian business facilities based on the 2012 Emilia-Romagna earthquake official database. *Bulletin of Earthquake Engineering*, 18: 1-29. 10.1007/s10518-019-00759-1

Sudret B. (2007). Uncertainty propagation and sensitivity analysis in mechanical models - Contributions to structural reliability and stochastic spectral methods; Hab. a diriger des recherches, Universite Blaise Pascal, Clermont-Ferrand, France.

Sudret B. (2008) Global sensitivity analysis using polynomial chaos expansions. *Reliability Engineering & System Safety*. 93(7): 964-979. 10.1016/j.ress.2007.04.002

Zhang Y, Burton HV, Sun H, Shokrabadi M. (2018). A machine learning framework for assessing post-earthquake structural safety. *Structural Safety.* 72: 1-16. 10.1016/j.strusafe.2017.12.001